JOURNAL OF VIROLOGY, Apr. 1977, p. 150-159
Vol. 22, No. 1

Printed in U.S.A.

Biophysical Studies of Infectious Pancreatic Necrosis Virus

PETER DOBOS,* ROSS HALLETT, DAVID T. C. KELLS, OLE SORENSEN, AND DAVID ROWE

Department of Microbiology, College of Biological Sciences, University of Guelph, Guelph, Ontario, NIG 2W1, Canada; Department of Physics, University of Guelph, Guelph, Ontario, NIG 2W1, Canada; and Department of Biochemistry, University of Toronto, Toronto, Ontario, M5S 1A1, Canada*

Received for publication 25 October 1976

The molecular weight of infectious pancreatic necrosis virus (IPNV) has been determined by analytical ultracentrifugation and dynamic light scattering. The sedimentation coefficient of the virus was found to be 435S. The average value for molecular weight is $(55 \pm 7) \times 10^6$. The virus genome consists of two segments of double-stranded RNA (molecular weights, 2.5×10^6 and 2.3×10^6), which represents 8.7% of the virion mass. The capsid protein moiety of IPNV consists of four species of polypeptides, as determined by polyacrylamide gel electrophoresis. The number of molecules of each polypeptide in the virion has been determined. There are 22 molecules of the internal polypeptide α (molecular weight, 90,000), 544 molecules of the outer capsid polypeptide β (molecular weight, 57,000), and 550 and 122 molecules, respectively, of the internal polypeptides γ_1 (molecular weight, 29,000) and γ_2 (molecular weight, 27,000). IPNV top component contains only the β polypeptide species, and its molecular weight is estimated to be 31×10^6. The hydrodynamic diameter and electron microscopic diameter (calculated by catalase crystal-calibrated electron microscopy) of IPNV was compared with those of reovirus and encephalomyocarditis virus. Due to the swelling of the outer capsid, reovirus particles were found to be much larger when hydrated (96-nm diameter) than when dehydrated (76-nm diameter), having a large water content and low average density. In contrast, IPNV particles are more rigid, having nearly the same average diameter under hydrous (64 nm) as under anhydrous conditions (59.3 nm). Encephalomyocarditis virus has a very low water content and does not shrink at all when prepared for electron microscopy.

Infectious pancreatic necrosis virus (IPNV) is the causal agent of a highly contagious and destructive disease of young hatchery-reared trout (31). The virus can be grown in tissue culture in a variety of established fish cell lines at an optimal temperature of 20 to 24°C (23, 31). Electron microscopic observations of purified virus revealed structures similar in size and shape to reovirus, but lacking the characteristic double capsid of the latter (6, 16). The virion polypeptides were shown to be distributed into three size classes of polypeptides of high (80,000), medium (50,000), and low (30,000) molecular weight (6). Recent studies indicated that the virus genome consists of two segments of high-molecular-weight double-stranded RNA (dsRNA) (2.5×10^6 and 2.3×10^6) (8, 21). The buoyant density of IPNV in CsCl gradients was found to be 1.33 g/cm^3 (10, 21), which indicated a lower RNA content than that of reovirus, which has a buoyant density of 1.36 g/cm^3 (12).

In contrast to the amount of information available on the biophysical properties of reovirus, there are no studies reported concerning the molecular weight of IPNV or its hydrodynamic behavior in aqueous buffer. This is largely due to the difficulty in obtaining milligram quantities of purified IPNV from infected cell cultures. For example, the yield of purified IPNV from tissue culture is at least 100 times less than that of purified reovirus (8). Consequently, it is not possible to determine the molecular weight of the virion by measuring the percent RNA content of purified virus preparations, a method that was used in earlier studies (13) to determine the molecular weight of reovirus.

An alternative procedure involves measurements of sedimentation coefficient (s), diffusion coefficients (D), and partial specific volumes ($\bar{v}$). The Svedberg equation (29) combines D, s, and $\bar{v}$ to yield the particle molecular weight; the Stokes-Einstein equation (29) relates D with the hydrodynamic diameter; and the molecular weight and the hydrodynamic diameter together yield the volume percentage of water of hydration. These methods also provide a means of relating properties of virus preparations in

solution with virus diameters and morphologies observed in electron micrographs. Of the above parameters, the most difficult term to measure is the diffusion coefficient, since boundary diffusion measurements in an analytical ultracentrifuge are time consuming and subject to large errors and require large amounts of purified virus. Without the diffusion coefficient, the other hydrodynamic measurements cannot be interpreted. The utilization of laser quasi-elastic light-scattering spectroscopy (LQELS) allows the measurement of D rapidly and with a precision of ±2% (12) on samples with concentrations in the readily available range of 10^8 to 10^{10} particles/ml (26). The use of LQELS made possible in recent years the determination of the molecular weight of a number of viruses, such as reovirus and reovirus cores (12, 15), Rous sarcoma virus and avian myeloblastosis virus (25), murine mammary tumor virus and feline leukemia virus (26), vesicular stomatitis virus and its defective particles (30), and various bacteriophages and bushy stunt virus (5).

In this paper we report the results of studies by LQELS on IPNV in comparison with reovirus and encephalomyocarditis (EMC) virus. Due to the relatively low particle concentrations of the IPNV preparations, the measurements of sedimentation coefficients were performed by the banding sedimentation velocity method, using a Vinograd-type cell in a Beckman model E ultracentrifuge equipped with UV scanning optics. In addition to the measurement of hydrodynamic properties of IPNV, we have also obtained negatively stained, catalase crystal-calibrated electron micrographs of the virus. This allowed us to directly compare the hydrodynamic diameters obtained by LQELS with diameters determined by electron microscopy. IPNV was found to have a sedimentation coefficient of 435S, and a molecular weight of 55×10^6 and to contain 8.7% RNA. By using these parameters together with polyacrylamide gel electrophoresis of proteins from purified virus, the number of different polypeptides per virion could also be calculated.

MATERIALS AND METHODS

Cell and virus. Rainbow trout gonad (RTG-2) cells and fathead minnow (FHM) cells were propagated as monolayers at 22°C in Corning plastic tissue culture flasks. The growth medium consisted of bicarbonate-buffered (pH 7.4) Eagle minimum essential medium (MEM) with Earle balanced salt solution supplemented with 10% fetal calf serum and 40 μg of gentamicin per ml. Mouse L cells were also grown in MEM at a temperature of 37°C.

The virus used in this study was the reference strain of IPNV (VR 299) obtained from the American Type Culture Collection. To propagate the virus, confluent RTG-2 or FHM cell monolayers were infected at a low multiplicity of infection to avoid the formation of defective interfering particles and incubated at 22°C for 2 to 4 days, and, after the development of extensive cytopathogenic effect, the free and cell-associated virus was concentrated and purified as described previously (8). The final step of purification consisted of CsCl isopycnic density gradient centrifugation. The gradient fractions containing infectious virus were pooled and diluted to 5 ml with TNE buffer (0.1 M Tris-0.1 M NaCl-0.001 M EDTA [pH 7.1]), and the virus was sedimented at 100,000 × g for 1 h at 5°C in a Beckman (L2-65B) preparative ultracentrifuge. The resulting pellet was resuspended in the appropriate buffer for each analysis, using a sonicating bath (Heat Systems-Ultrasonics Inc.). For hydrodynamic studies the virus pellet was resuspended in only 200 μl of TNE buffer because of the low particle concentration of the virus. IPNV purified from 10^9 infected cells had an optical density at 260 nm (OD_{260}) of 0.2/ml, representing 40 μg of virus or 10^{10} to 10^{11} particles/ml, using the formula of Smith et al. (28) for reovirus (1 $OD_{260} = 2.1 \times 10^{12}$ particles or 200 μg of virus). Plaque assay of IPNV was performed according to a previously described method (9).

The preparation of ^{32}P-labeled purified IPNV and the method of RNA extraction have been described previously (8).

The growth and purification of ^{14}C-amino acid-labeled or [^{35}S]methionine-labeled virus were also performed according to a previously described method (10).

EMC virus was grown in mouse L cell monolayers and purified by the method of Kerr and Martin (18). Reovirus type 3 was also propagated in L cells and purified by the method of Smith et al. (28).

dsRNA extracted from bacteriophage φ6 was the generous gift of A. L. Vidover and J. L. Van Etten of the University of Nebraska.

Polyacrylamide gel electrophoresis of viral RNA. The method of Reddy and Black (24) was used to analyze labeled IPNV RNA in 7.5 and 5% acrylamide gels. Unlabeled reovirus RNA and φ6 dsRNA served as molecular weight markers. A detailed description of the electrophoretic procedure and subsequent autoradiography has been published recently (8).

Polyacrylamide gel electrophoresis of viral polypeptides. [^{35}S]methionine-labeled, ^{14}C-amino acid-labeled, and unlabeled IPNV polypeptides were analyzed in 10 and 12% discontinuous acrylamide slab gels, using a Tris-glycine buffer system developed by Laemmli (20), as well as in 7.5 and 10% cylindrical sodium dodecyl sulfate (SDS)-phosphate gels, as described by Maizel (22). The molecular weights of virion polypeptides were determined by comparing their electrophoretic mobilities to polypeptides of reovirus, EMC virus, phosphorylase A, bovine serum albumin, ovalbumin, and tobacco mosaic virus. The conditions of electrophoresis and subsequent processing of gels have been described previously (10).

Determination of diffusion coefficients. In quasi-elastic light scattering, the value of D is usually calculated from the slope of a semilogarithmic plot

of the electric field autocorrelation function of the scattered light. The method has been fully discussed elsewhere (1, 7) and is ideally suited to the measurements of the diffusion coefficients of nearly spherical viruses. The particular device used in this research is similar to most other photon correlation systems (15, 25), with the exception that the full-intensity autocorrelation function $g_2(\tau)$ is calculated by an on-line NOVA-2 minicomputer (14). The minicomputer also contains a program that, by the least-squares method, fits a third-order polynomial to $ln\, g_2(\tau)$ and relates the coefficients of the best-fit polynomial to the cumulants of the distribution of scatterers by the methods of Koppel (19) and Kendall and Stuart (17).

In this study our interest was on the first cumulant, which yields the average correlation time τ_c associated with light scattered from the sample. For the nearly spherical virus sample studies, τ_c is related to the average diffusion coefficient by:

$$D = \frac{1}{\tau_c K^2} \quad (1)$$

where K is the scattering vector given by:

$$K = \frac{4\pi n}{\lambda} \sin\frac{\theta}{2} \quad (2)$$

In this equation n is the refractive index of the solution, λ is the vacuum wavelength of the laser light used (632.8 nm), and θ is the scattering angle. All measurements were carried out at a scattering angle of 90°. By using this approach, we were able to obtain the diffusion coefficient of a particular virus sample as well as some idea of its monodispersity.

Since the samples were maintained at 20 ± 0.2°C throughout the light-scattering experiments, a viscosity correction was required only to obtain $D^\circ_{20,w}$ values (the buffer solution used has a relative viscosity of 1.1287 at 20°C, as measured with a Brookfield rotating cone microviscometer).

Particle concentrations for all virus preparations were estimated to be about 10^{11} particles/ml, so that number fluctuations were not expected and, indeed, did not contribute to the intensity autocorrelation functions. The statistical uncertainty in the values of τ_c was found, on the basis of 10 identical experiments, to be ±2.0% (1 standard deviation). This, combined with uncertainties in temperature and viscosity, led to a total uncertainty of $D^\circ_{20,w}$ of ±2.5%.

The major potential source of error in the measurement of diffusion coefficients is the presence of aggregates in the purified suspension of virus particles. Initial preparations of virus were found to give inconsistent results when the virus was pelleted and resuspended in TNE buffer. This problem has been overcome by brief sonic treatment of the sample (20 to 30 s). The resulting preparation sedimented as a single band when examined by UV scanning optics in an analytical ultracentrifuge, indicating the monodispersity of virus particles.

Sedimentation analysis. To determine the sedimentation coefficient of the virus, banding sedimentation velocity experiments were performed in a Beckman model E ultracentrifuge equipped with UV scanning optics. A four-place AnK rotor and 30-mm Vinograd type III cells were used at a rotor speed of 9,000 rpm. Ten to twenty microliters of 0.2 OD_{260} solutions of the virus was layered onto a bulk sedimentation solvent in TNE buffer prepared in 99.7% D_2O. Solvent densities were measured in a Parr digital precision density meter, and solvent viscosities were measured in a Cannon-Ubbelohde semi-microdilution viscometer, which has a flow time for water of 275 s. All experiments were performed at 20°C.

Determination of $\bar{v}$. The partial specific volume ($\bar{v}$) is the volume of water displaced by 1 g of the virus in a dilute aqueous salt solution. It enters into the Svedberg equation as the factor $(1 - \bar{v}\rho)$, where ρ is the density of the solution; thus, the determination of the density of a solution in which the sedimentation coefficient is equal to 0 gives a measure of $\bar{v}$. Accordingly, the sedimentation rate of the virus is measured in a series of solutions of increasing density, and the resulting data are plotted in a manner to enable extrapolation to the value of ρ, corresponding to a 0 sedimentation rate. This value for the density of the solution is equal to $1/\bar{v}$. Since the equation is restricted to two-component systems, it is not valid to employ a third component (e.g., sucrose) to increase the density of the solution (27). However, mixtures of D_2O and water act as a one-component solvent and can be used for these experiments. The drawback of this method is that D_2O solutions are not sufficiently dense to reduce the sedimentation rate of viruses to 0, and extrapolation of the data is necessary. With accurate data, however, this can be performed to yield reliable results, and the method has been used to determine the molecular weights of a number of different viruses (4, 5).

To determine $\bar{v}$ of IPNV, sedimentation experiments were carried out with the virus in TNE buffers nominally containing 50, 70, 90, and 100% D_2O. Apparent sedimentation coefficients (s_{app}) were calculated from the radial displacement of the peak maxima, using linear least squares. The viscosities and densities of the sedimentation solvents were measured. Values of $(s_{app}\,\eta/\eta_o)$ were plotted against ρ, the solvent density, and the partial specific volume $\bar{v}$ was obtained as the reciprocal of the intercept at $(s_{app}\,\eta/\eta_o) = 0$ by a least-squares procedure. In this calculation the apparent sedimentation coefficients were weighted with the reciprocals of the variances obtained from the calculation of the sedimentation coefficients.

Molecular weight determination. The molecular weights of the virus particles were obtained from their hydrodynamic parameters by means of the Svedberg equation:

$$M = s^\circ_{20,w}\, RT/D^\circ_{20,w}\,(1 - \bar{v}\rho) \quad (3)$$

where M is the molecular weight; $s^\circ_{20,w}$ and $D^\circ_{20,w}$ are the sedimentation and diffusion coefficients in water at 20°C, extrapolated to a zero concentration; $\bar{v}$ is the partial specific volume; R is the gas constant; T is the absolute temperature; and ρ is the density of water. The statistical errors associated with the parameters in this equation were combined

according to the approximation (see equation 4) to obtain an uncertainty in M (2).

$$\sigma_M^2 \simeq \sigma^2_{s^\circ_{20,w}} \left(\frac{\partial M}{\partial s^\circ_{20,w}}\right)^2 + \sigma_T^2 \left(\frac{\partial M}{\partial T}\right)^2 + \sigma^2_{D^\circ_{20,w}} \left(\frac{\partial M}{\partial D_{20,w}}\right)^2 + \sigma_{\bar{v}}^2 \left(\frac{\partial M}{\partial \bar{v}}\right)^2 \quad (4)$$

Typically, this uncertainty was in the order of 14%, contributed mostly by the uncertainty in the partial specific volume.

Electron microscopy. Carbon support films were prepared by carbon-coated, collodion-coated 400-mesh grids. The collodion was then removed with amyl acetate.

Negative stains were prepared with glass-distilled water and filtered through a membrane filter (0.22 μm; Millipore Corp.) prior to use. Samples were stained with either 1% uranyl acetate, pH 4.2, or 2% phosphotungstic acid, pH 1.4.

The catalase crystal suspension used in this experiment was kindly donated by Nicholas G. Wrigley and prepared as described by Wrigley (32).

Concentrated virus or virus top component was applied to the carbon film in a 10-μl drop. The excess was removed after 30 s, and a 10-μl drop of suspended catalase was then applied. After 15 s, the excess was removed and 20 μl of the appropriate stain was added. The excess stain was removed after 30 s, and the grid was allowed to air-dry.

Specimens were observed as soon after preparation as possible with a Philips EM300 operated at 60 kV.

The crystallographic repeat distance of 8.8 ± 0.3 nm of added catalase crystals was used as an internal size calibration (32).

Enzymes, chemicals, and isotopes. Eagle MEM and fetal calf serum (virus and mycoplasma screened) were purchased from Grand Island Biological Co.; gentamicin from Microbiological Associates; SDS, specially pure, and proteinase K from B.D.H. Ltd.; and RP/R-2 Royal X-omat film from Kodak. Electrophoresis grade acrylamide, *N,N'-O*-methylenebisacrylamide, and *N,N,N',N''*-tetramethylethylenediamine were purchased from Bio-Rad Laboratories; [^{32}P]orthophosphoric acid (carrier-free), 2,5-diphenyloxazole, 1,4-bis-[2]-(5-phenyloxazolyl)benzene, [^{35}S]methionine (400 Ci/mmol), and U-^{14}C-labeled amino acid mixture (0.1 mCi/ml) were the products of New England Nuclear Corp.

RESULTS

Virus genome. Earlier studies indicated that the genome of IPNV is single-stranded RNA (16). However, recent reports from a number of laboratories have shown the virus to contain two segments of high-molecular-weight dsRNA (6, 9, 21). The analysis of ^{32}P-labeled viral RNA together with unlabeled reovirus RNA and phage φ6 RNA on a 7.5% acrylamide gel is shown in Fig. 1. When the relative electrophoretic mobility of IPNV RNA was plotted against those of the marker RNAs, the molecular weights of the two genome segments were found to be 2.5 × 10^6 and 2.3 × 10^6, respectively. The same results were observed with low- and high-passage virus or when IPNV was grown in FHM cells instead of RTG-2 cells. Care was taken to infect cells at a low multiplicity (0.1 to 1.0 PFU/cell); therefore, it is unlikely that the smaller of the two RNA segments (2.3 × 10^6 daltons) is due to the presence of defective interfering particles. Furthermore, melting and reannealing of the viral dsRNA did not result in the formation of a hybrid dsRNA molecule of intermediate molecular weight (data not shown), indicating that the two genome segments have different nucleotide sequences.

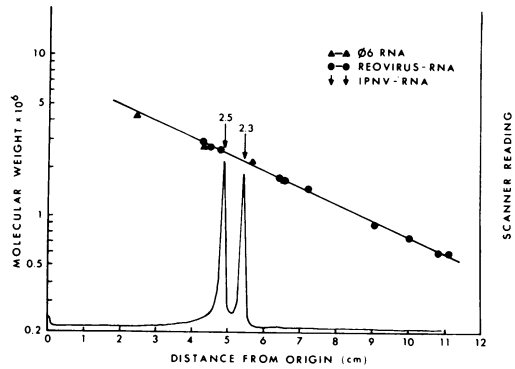

FIG. 1. *Acrylamide gel electrophoresis of ^{32}P-labeled IPNV RNA analyzed together with unlabeled reovirus RNA and phage φ6 RNA in a 7.5% cylindrical gel. The photograph of the strained gel pattern was superimposed on the autoradiogram to determine the molecular weight of the two dsRNA segments of the virus genome (indicated by arrows; 2.5 × 10^6 and 2.3 × 10^6). The densitometer tracing of the autoradiogram shows the relative distribution of radioactivity in the two genome segments.*

Virus polypeptides. When freshly purified IPNV was analyzed by SDS-acrylamide gel electrophoresis, the polypeptide pattern shown in Fig. 2A was obtained. The virus contains three size classes of polypeptides: the high-molecular-weight but least abundant α polypeptide (90,000), the medium sized and most abundant β polypeptide (57,000), and two low-molecular-weight γ polypeptides (γ_1 major, 29,000, and γ_2 minor, 27,000).

The α polypeptide showed two components if the virus was stored (−20°C) before analysis on acrylamide gels (Fig. 2B), indicating either proteolytic degradation of α or, alternatively, dimerization of β.

Polypeptides α and γ of the virion were not detected in top component preparations (Fig. 2C). Purified [^{35}S]methionine-labeled top component revealed a single polypeptide that comi-

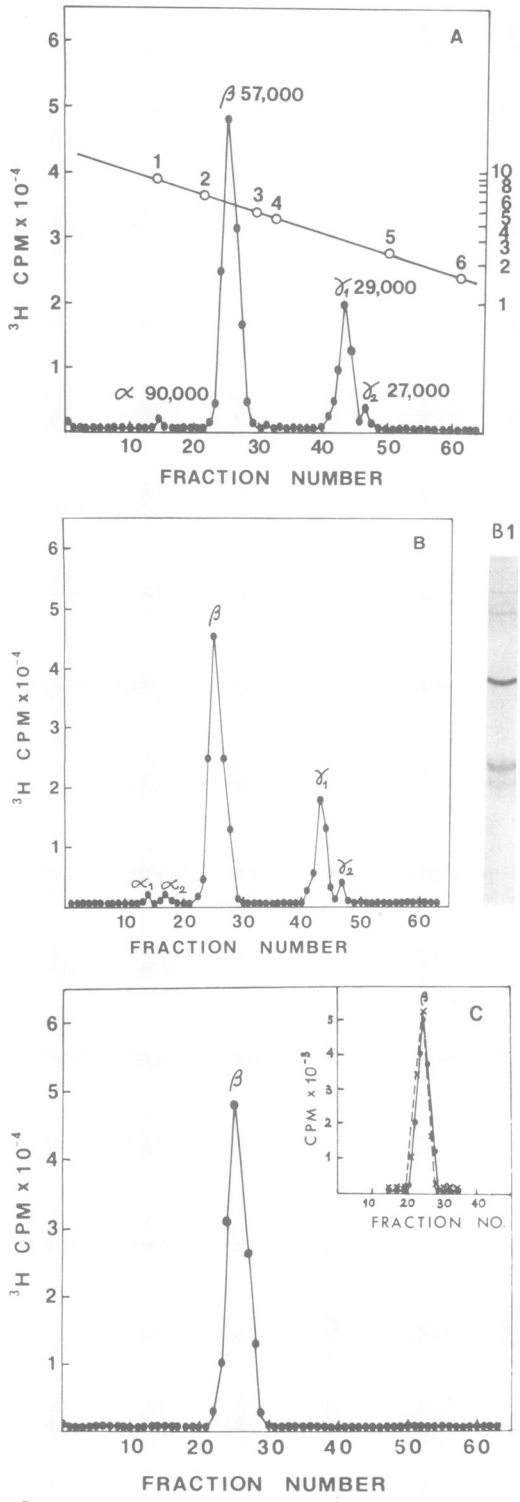

FIG. 2. *Polypeptide composition of IPNV. Purified virus labeled with a mixture of ^{3}H-amino acids was dissociated by heating in electrophoresis sample buffer, and the proteins were analyzed in 7.5% SDS-phosphate acrylamide gels together with marker proteins of known molecular weights. After electrophoresis, the gels were stained with 0.1% Coomassie brilliant blue and destained in 7% acetic acid, and the positions of the marker proteins were established by scanning the gels with a chromoscan recording microdensitometer. The radioactivity in gel fractions was measured as described in the text. (A) Electrophoretic profile of freshly prepared IPNV. Numbers 1 to 6 indicate the positions of marker proteins: 1, phosphorylase A; 2, bovine serum albumin; 3, γ globulin H chain; 4, ovalbumin; 5, γ globulin L chain; and 6, tobacco mosaic virus protein (reovirus and EMC virus proteins were also used as markers, but were omitted here for the sake of clarity). The label on the right indicates the logarithmic scale of molecular weights. (B) Electrophoretic profile of purified IPNV that had been stored at −20°C in electrophoresis sample buffer prior to analysis. (B1) Autoradiogram of stored virus labeled with a mixture of ^{14}C-amino acids. (C) Electrophoretic profile of IPNV top component. (Inset) Co-electrophoresis of [^{35}S]methionine-labeled top component (×) and ^{3}H-amino acid-labeled virus (●). (Only the β region of the gel is plotted.)*

grated in acrylamide gel with the β protein of differentially labeled virion (Fig. 2C, inset), indicating that top component contains only β protein. Electron micrographs of IPNV top component (Fig. 3C) show empty virus particles. Taken together, these results suggest that the outer capsid is made up of β polypeptides and that polypeptides α and γ are probably internal proteins closely associated with the virus genome.

The percent distribution of the different virion polypeptides (calculated from a number of gel profiles) is presented in Table 3.

Sedimentation coefficient and partial specific volume. The concentration dependence of the sedimentation coefficient of the virus was examined by layering 10, 15, and 20 μl of the stock solution (OD_{260} = 0.2) onto the nominal 100% D_2O sedimentation solvent. The apparent sedimentation coefficients, weighted with the reciprocals of their variances, were plotted as a function of concentration, and the results were extrapolated to zero concentration. From this calculation, the value of s°_{20} = 248.49 ± 0.11*S* was obtained. The effects of solvent viscosity and density were removed by using the usual equation to yield a corrected sedimentation coefficient of 435 ± 42*S*. The major part of the uncertainty in this quantity is due to the uncertainty in the partial specific volume.

The partial specific volume of virus particles was determined by sedimentation in mixtures of D_2O and water containing the components present in TNE buffer. The apparent sedimentation coefficients, solvent viscosities, and densities in the two-component system, con-

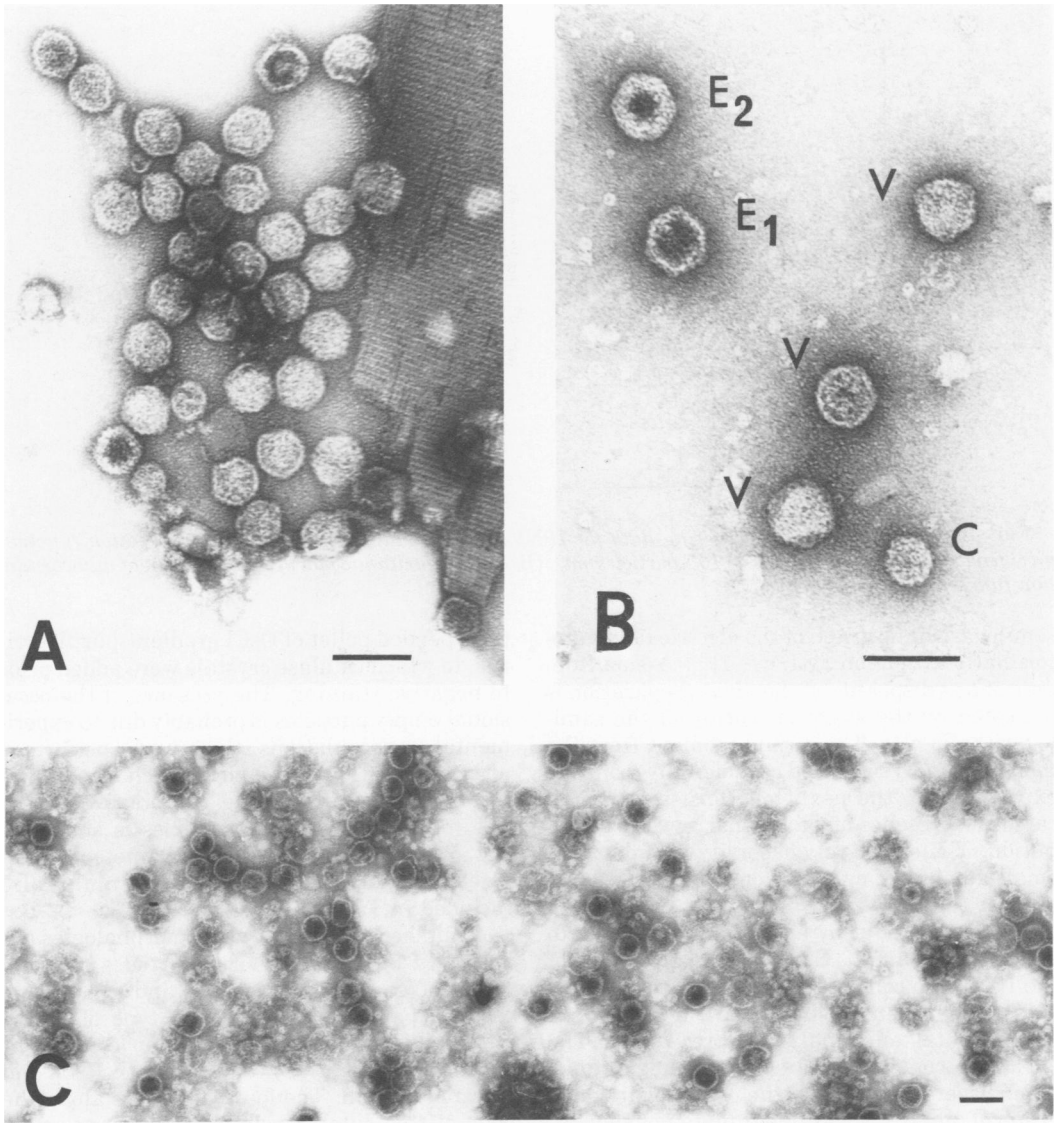

FIG. 3. *Electron micrographs of uranyl acetate-stained IPNV. (A) Low magnification (×103,500) together with catalase crystals. (B) Higher magnification (×128,200), showing full virus particles (V), a corelike particle (C), and two kinds of empty particles (E_1 and E_2). (C) Low magnification (×54,200) of top component preparation. Note empty particles, broken capsids, and individual capsomers. Bar = 100 nm.*

taining different proportions of D_2O are shown in Table 1. The measured value of $\bar{v}$ for virus particles was found to be 0.7065 ± 0.0554 ml/g according to the calculation described above.

Diffusion coefficient and hydrodynamic diameter. An intensity autocorrelation function $[g_2(\tau)]$ obtained from the IPNV preparation is shown in Fig. 4A. Application of the moments analysis to this function yielded an average value of τ_c of 483 μs. Using equation 1 and the correlation for solvent viscosity leads to a value of $D^\circ_{20,w}$ of 6.7 × 10^{-12} m^2/s. Figure 4B is a

TABLE 1. *Calculation of partial specific volume*

D_2O (%)	Apparent sedimentation coefficient		Solvent viscosity (n/n_o, 20°C)	Solvent density (ρ, g/cm^3)
	s_{app}, 20°C (S)	Standard error (S)		
50	321.95	±3.85	1.1414	1.0566
70	288.20	±1.76	1.1909	1.0780
90	257.68	±1.56	1.2422	1.0994
100	244.16	±1.76	1.2779	1.1106

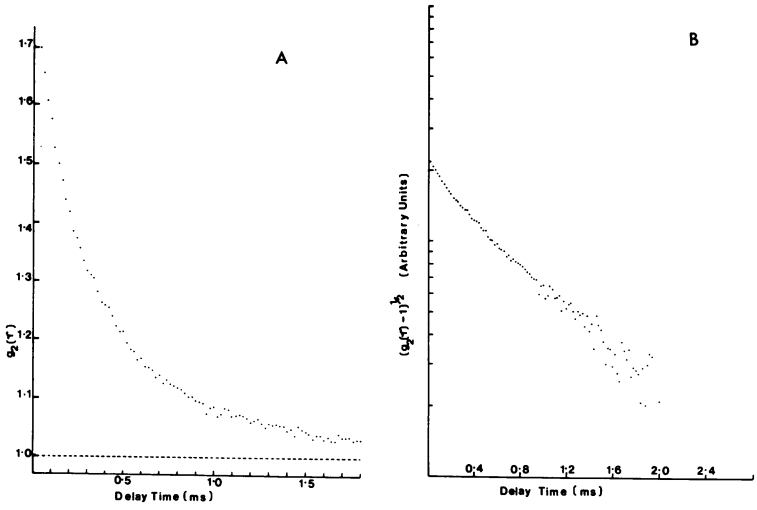

FIG. 4. *Experimental light-scattering data for IPNV. (A) Normalized intensity autocorrelation function $g_2(\tau)$ from a suspension of virus (~10^{10} particles/ml). (B) Semilogarithmic plot of the electric field autocorrelation function shown in (A).*

semilogarithmic graph of the electric field autocorrelation function $[g_2(\tau) - 1]^{1/2}$. A small degree of polydispersity of the virus preparation is indicated by the slight curvature of the semilogarithmic plot. The second moment from the moments analysis varied considerably from one experiment to the next, but consistently indicated the presence of a fairly narrow size distribution. The slight polydispersity was due to a small amount of aggregation. Thus, the value of τ_c for the IPNV may be slightly higher than the true value, but by an amount estimated to be no more than 5%. Studies were also made of the IPNV top component, EMC virus, and reovirus, the latter serving as a control for our experimental and analytical procedures. The IPNV top component sample was judged to be monodisperse because the semilogarithmic graph of $\sqrt{g_2(\tau) - 1}$ was linear (data not shown).

The hydrodynamic diameter (d) of the particles may be derived from their measured diffusion coefficients by using the Stokes-Einstein equation: $D = (kT)/(3\ \pi\eta d)$, where D is the diffusion coefficient, k is the Boltzman constant, T is the absolute temperature, and η is the viscosity of the solution. The results are tabulated in Table 2. The values for the diffusion coefficients and the hydrodynamic diameter of reovirus agree well with previous studies (9). The results also indicate that in aqueous buffer the IPNV top component was slightly larger than the intact virus.

Electron microscopy. A low-magnification electron micrograph of IPNV and added catalase crystals, used for internal size calibration, is shown in Fig. 3A. The virus shown is a resuspended pellet of CsCl gradient-purified virus, to which catalase crystals were added prior to negative staining. The presence of the occasional empty particles is probably due to experimental manipulations that were performed after purification of the virus, such as repelleting and sonically treating the preparation. A size histogram of single particles is shown in Fig. 5; the arithmetic average diameter is indicated by an arrow. This value (59.3 nm) is also included in Table 2.

A number of different virus morphologies are shown in Fig. 3B: full virus particles (V), two kinds of empty particles (E_1 and E_2), and a corelike particle (C). E_1 is the type of empty particle that can be found in top component preparations (Fig. 3C) that lack both RNA and internal protein. The four capsomers along the edge of this outer capsid shell are readily observable. The size of the inside cavity in these particles (diameter, 40 to 45 nm) corresponds to the size of the corelike particle (C) that has only three capsomers along one edge of the icosahedron. The other type of empty particle (E_2) seems to have lost only the viral genome, but not the core proteins.

Particles found in top component preparations (ρ = 1.29 g/cm^3) are shown in Fig. 3C. These are heterogenous in size since many of the empty particles show broken or damaged capsid shells in various degrees of distortion. Due to the heterogeneity of the preparation, size determinations were not performed on these particles.

The electron microscopic diameter of purified EMC virus was determined to be 28.5 nm, using

TABLE 2. *Hydrodynamic properties and electron microscopic diameters of reovirus, IPNV, and EMC virus together with their molecular weights as calculated from the Svedberg equation*[a]

Particle	$D^{\circ}_{20,w}$ (m^2/s)	$s_{20,w}$	$\bar{v}$	Hydrodynamic diam (nm)[b]	Electron microscopic diam (nm)	Equivalent solid particle diam (nm)[c]	Water content (ml/g of particle)	Volume % water	Avg particle density (g/ml)[d]	Mol wt avg
Reovirus	4.4×10^{-12}	734[e]	0.690[e]	96.0	76	65.6[f]	1.5[f]	68	1.14[f]	129.5×10^{6}[e]
IPNV	6.7×10^{-12}	435	0.706	64.0	59.3	49.7	0.8	53	1.20	55×10^{6}
IPNV top component	5.0×10^{-12}			84.0						31×10^{6}[g]
EMC virus	16.0×10^{-12}[h]	162	0.678[i]	26.7[h]	28.0	26.2	<0.2[j]	27	1.40	8.1×10^{6}

[a] The estimated errors in the above results are as follows: diffusion coefficient (±2.5%), $s_{20,w}$ (±9.6%), $\bar{v}$ (±7.8%), hydrodynamic diameter (±2.5%), electron microscopic diameter (±2.4%), equivalent solid particle diameter (±5%), water content (±10%), percent volume of water (±11%), and molecular weight (±14%). The percent error in molecular weight determinations was contributed by the errors associated with the parameters of the Svedberg equation and calculated by using equation 4.

[b] Hydrodynamic diameters were determined from measured diffusion coefficients.

[c] The equivalent solid particle diameters were determined from molecular weights, particle specific volumes, and the volume of the particle.

[d] The particle densities were calculated from the total mass of the particle (anhydrous molecular weight plus bound water) and the volume of the particle, assuming a density of 1 g/ml for water.

[e] As determined by Farrel et al. (12).

[f] As determined by Harvey et al. (15).

[g] As determined from the percentage of virion protein represented by the top component polypeptides (see Table 3).

[h] The estimated errors for EMC virus of $D_{20,w}$, ± 5%, and hydrodynamic diameter, ± 5%.

[i] As determined by Burness and Clothier (4).

[j] Because of the similarity in magnitude of d_h and d_s, the uncertainty in the absolute magnitude of the water content is very large; however, error analysis suggested that the 0.2 value quoted is a reasonable upper limit.

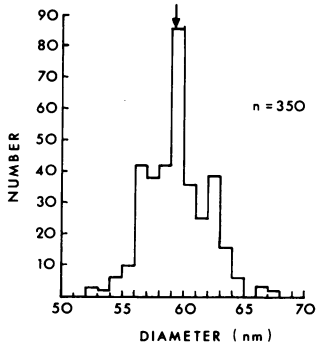

FIG. 5. *Size histogram of IPNV particles determined from electron micrographs, such as shown in Fig. 3A, containing catalase crystals for internal calibration. The arrow indicates the arithmetic average diameter. n is the total number of particles measured.*

catalase crystals as internal markers (Table 2).

Molecular weight and water content of virus particles. The molecular weight of IPNV, using equation 3, was found to be $55 \times 10^6 \pm 7 \times 10^6$ (Table 2). The degree of uncertainty of this figure (14%) was calculated by using equation 4. Most of this value was contributed by the uncertainty in the partial specific volume. The hydrated diameter of reovirus is 20 nm larger than its electron microscopic diameter (9) due to the swelling of the outer capsid in aqueous buffer. The hydrated diameter of IPNV and EMC virus, on the other hand, differs little from the electron microscopic diameter, suggesting that little, if any, shrinkage of the particles occurs during the fixation and dehydration procedures involved in the preparation of specimens for electron microscopy. Neither of these viruses possesses the type of outer capsid present in reovirus particles.

The water content of virus particles may be calculated from the hydrated diameter (d_h), equivalent solid particle diameter (d_s), and partial specific volume ($\bar{v}$) from the formula: $w = [(d_h^3 - d_s^3)/d_s^3]\bar{v}$ ml/g of particle.

The water contents calculated in this way for the various viruses are shown in Table 2. The volume percentage of water can be estimated by the formula: % water $= [(d_h^3 - d_s^3)/d_h^3] \times 100$.

DISCUSSION

The results presented in this paper show that the IPNV capsid consists of four polypeptides that fall into three size classes. The molecular weights of these polypeptides, their relative contribution to virion mass, and the number of molecules of each species per virion are given in Table 3.

These estimates are based on the findings

TABLE 3. *Summary of IPNV capsid proteins*[a]

Suggested location	Designation	Mol wt	% in virion	Approx no. of molecules/virion[b]
Internal protein	α	90,000	4	22
Outer capsid	β	57,000	62	544
Internal protein	γ_1	29,000	28	550
Internal protein	γ_2	27,000	6	122

[a] The molecular weights of IPNV polypeptides were determined by comparing their electrophoretic mobilities in SDS-polyacrylamide gels with proteins of known molecular weights. The following marker proteins were used: reovirus proteins as characterized by Both et al. (3), EMC virus proteins as characterized by Dobos and Martin (11), bovine serum albumin (67,000), phosphorylase A (90,000), globulin H chain (50,000), ovalbumin (45,000), globulin L chain (25,000), and tobacco mosaic virus protein (17,500). The values are the averages of 12 determinations.

[b] Obtained by dividing the percentage of a given polypeptide (expressed in daltons) by the molecular weight of the polypeptide.

that the molecular weight of IPNV is 55×10^6 and the virion contains 8.7% RNA (4.8×10^6). This leads to an estimate of 50.2×10^6 daltons for the total weight of the capsid protein. The outer shell is made up of 92 capsomers (6, 16) and is estimated to contain 544 β polypeptide molecules; these figures indicate that a single capsomer is made up of 6 β polypeptide chains, except in the case of 12 pentamers that constitute the apexes of the icosahedron (80 hexamers contain $80 \times 6 = 480$ β polypeptides, and the 12 pentamers contain $12 \times 5 = 60$ β polypeptides, a theoretical total of 540 β protein molecules, assuming that the vertexes of the icosahedron are constructed of the same protein as is the rest of the shell). Our previous studies (10) indicated the presence of two high-molecular-weight polypeptides in the virion (α_1 and α_2). This has been observed in both purified virus preparations and isotopically labeled infected cells that have been stored in electrophoresis sample buffer at −20°C. Freshly prepared material contained only one α polypeptide, which could not be separated into two components, even by using 30-cm-long acrylamide gels. Therefore, we conclude that the additional α protein was an artifact, arising either by proteolytic degradation of α_1 or through dimerization of polypeptide β.

Polypeptides γ_1 and γ_2 are so close in molecular weight that one may conceivably have been derived as a cleavage product of the other; if this turns out to be the case, then the data in Table 3 will require reinterpretation. IPNV top component contains only polypeptide β (Fig. 2C). In our previous study (10) an additional protein of slightly higher molecular weight was also detected, which was found only in infected cells and seemed to be the precursor of the β polypeptide. This additional precursor molecule also bands at a buoyant density of 1.29 g/cm^3 and can be removed by sedimenting the CsCl-banded top component preparation through a column of sucrose before analysis in acrylamide gels.

Electron micrographs of top component preparations show empty particles, with a single capsid layer that contains only the β protein. Taken together, these results suggest that the α and γ polypeptides are internal proteins. This is in marked contrast to the situation found in reovirus preparations, in which the polypeptides in reovirus top component are identical with those of virions.

Particles that appeared to be IPNV cores (Fig. 3B) were only observed in pelleted material (regardless of whether it was a semipurified virus pellet or isopycnically banded virus that was pelleted subsequently) and not in virus banded in CsCl gradients. This seemed to indicate that the corelike particles were the result of pelleting or subsequent resuspension of virus preparations. We were unsuccessful in rebanding them in cesium chloride gradients and could not prepare them from purified virus by applying the method used to prepare reovirus cores in vitro (28). The dimensions of the corelike particles of IPNV are identical to the cavities of top components, giving further support to the theory that these particles are indeed virus cores; nevertheless, further studies are needed to settle this point.

Our results on the hydrodynamic diameter of reovirus are in excellent agreement with those of Farrel et al. (12), indicating that the outer capsid of reovirus swells in aqueous buffers, resulting in a hydrodynamic diameter of 96 nm, which is 20 nm greater than that observed by electron microscopy. In contrast, the hydrodynamic diameter of IPNV is only slightly larger than its anhydrous diameter (Table 2), indicating that these particles shrink very little when dehydrated in preparation for electron microscopy. The difference (4.7 nm) of the two diameters is within the combined experimental error in the electron microscopic and light-scattering techniques. The differences between the two viruses are also reflected in their water content and average particle densities. Neither reovirus nor IPNV shrinks as far as its limiting solid particle diameter.

EMC virus was included in these hydrodynamic measurements for comparison, since this virus does not possess a double capsid and most of its biophysical characteristics are already established (4). The diffusion coefficient, as determined by light scattering, is slightly higher (Table 2) than the values obtained by equilibrium centrifugation (4), and this results in a virion molecular weight that is slightly lower than previous estimates. Similar to the results of Burness and Clothier (4), we have found that the hydrodynamic and electron microscopic diameters of EMC virus are virtually the same (Table 2), indicating that the virus particles have a very low water content and do not shrink at all when prepared for electron microscopy. In this respect EMC virus behaves like the rigid, dense reovirus core particle, which also has a low water content and, as shown by Harvey et al. (15), does not shrink upon dehydration.

These results show that by using the LQELS method in combination with analytical ultracentrifugation, acrylamide gel electrophoresis, and electron microscopy, viruses can be well characterized, even when they are available only at low particle concentrations.

ACKNOWLEDGMENTS

We gratefully acknowledge financial support of the National Research Council of Canada.

We are also thankful to Jackie Marsh for skillful technical assistance.

LITERATURE CITED

1. **Berne, B. J., and R. Pecora.** 1976. Dynamic light scattering. John Wiley & Sons, Inc., New York.
2. **Bevington, P. R.** 1969. Data reduction and error analysis for the physical sciences, p. 56–65. McGraw-Hill Book Co., New York.
3. **Both, G. W., S. Lavi, and A. J. Shatkin.** 1975. Synthesis of all the gene products of the reovirus genome *in vivo* and *in vitro*. Cell 4:173–180.
4. **Burness, A. T. H., and F. W. Clothier.** 1970. Particle weight and other biophysical properties of encephalomyocarditis virus. J. Gen. Virol. 6:381–393.
5. **Camerini-Otero, R. D., P. N. Pusey, D. E. Koppel, D. W. Schafer, and R. M. Franklin.** 1974. Intensity fluctuation spectroscopy of laser light scattered by solutions of spherical viruses. R-17, QB, BSV, PM_2 and T-7. II. Diffusion coefficients, molecular weights, solvation and particle dimensions. Biochemistry 13:960–970.
6. **Cohen, J., A. Poinsard, and R. Scherrer.** 1973. Physicochemical and morphological features of infectious pancreatic necrosis virus. J. Gen. Virol. 21:485–498.
7. **Cummins, H. Z., and E. R. Pike (ed.).** 1974. Photon correlation and light beating spectroscopy. Plenum Press, New York.
8. **Dobos, P.** 1976. Size and structure of the genome of infectious pancreatic necrosis virus. Nucleic Acid Res. 3:1903–1924.
9. **Dobos, P.** 1976. Use of gum tragacanth overlay, applied at room temperature, in the plaque assay of fish and other animal viruses. J. Clin. Microbiol. 3:373–375.
10. **Dobos, P.** 1977. Virus-specific protein synthesis in cells infected by infectious pancreatic necrosis virus. J. Virol. 21:242–258.
11. **Dobos, P., and E. M. Martin.** 1972. Virus-specific polypeptides in ascite cells infected with encephalomyocarditis virus. J. Gen. Virol. 17:197–212.
12. **Farrel, J. A., J. D. Harvey, and A. R. Bellamy.** 1974. Biophysical studies of reovirus type 3. I. The molecular weight of reovirus and reovirus cores. Virology 62:145–153.
13. **Gomatos, P. J., and I. Tamm.** 1963. The secondary structure of reovirus RNA. Proc. Natl. Acad. Sci. U.S.A. 49:707–714.
14. **Gray, A. L., F. R. Hallett, and A. Rae.** 1975. Digital autocorrelation by minicomputer. J. Phys. E 8:501–506.
15. **Harvey, J. D., J. A. Farrell, and A. R. Bellamy.** 1974. Biophysical studies of reovirus type 3. II. Properties of the hydrated particle. Virology 62:154–160.
16. **Kelly, R. K., and P. C. Loh.** 1972. Electron microscopical and biochemical characterization of infectious pancreatic necrosis virus. J. Virol. 10:824–834.
17. **Kendall, M. G., and A. Stuart.** 1958. The advanced theory of statistics, vol. 1. Charles Griffen and Co. Ltd., London.
18. **Kerr, I., and E. M. Martin.** 1972. Simple method for the isolation of encephalomyocarditis virus ribonucleic acid. J. Virol. 9:559–561.
19. **Koppel, D. E.** 1972. Analysis of macromolecular polydispersity in intensity correlation spectroscopy: the method of cumulants. J. Chem. Phys. 57:4810–4820.
20. **Laemmli, U. K.** 1970. Cleavage of structural proteins during the assembly of the head of bacteriophage T_4. Nature (London) 227:680–685.
21. **Macdonald, R. D., and T. Yamamoto.** 1976. The structure of infectious pancreatic necrosis virus RNA. J. Gen. Virol. 34:1–13.
22. **Maizel, J. V., Jr.** 1971. Polyacrylamide gel electrophoresis of viral proteins, p. 180–247. *In* K. Maramorosch and H. Koprowski (ed.), Methods in virology, vol. 5. Academic Press Inc., New York.
23. **Malsberger, R. G., and C. P. Cerini.** 1965. Multiplication of infectious pancreatic necrosis virus. Ann. N.Y. Acad. Sci. 126:320–327.
24. **Reddy, D. V. R., and L. M. Black.** 1973. Electrophoretic separation of all components of the double-stranded RNA of wound tumor virus. Virology 54:557–562.
25. **Salmeen, I., L. Rimai, L. Liebes, M. A. Rich, and J. J. McCormick.** 1975. Hydrodynamic diameters of RNA tumor viruses: studies by laser beat frequency spectroscopy of avian myeloblastosis and Rauscher murine leukemia viruses. Biochemistry 14:134–141.
26. **Salmeen, I., L. Rimai, R. B. Luftig, L. Liebes, E. Retzel, M. Rich, and J. J. McCormick.** 1976. Hydrodynamic diameters of murine mammary, Rous sarcoma, and feline leukemia RNA tumor viruses: studies by laser beat frequency light-scattering spectroscopy and electron microscopy. J. Virol. 17:584–596.
27. **Schachman, H. K.** 1957. Ultracentrifugation, diffusion and viscometry, p. 32–104. *In* S. P. Colowick, and N. O. Kaplan (ed.), Methods in enzymology, vol. 4. Academic Press Inc., New York.
28. **Smith, R. E., H. J. Zweerink, and W. K. Joklik.** 1969. Polypeptide components of virions, top component and cores of reovirus type 3. Virology 39:791–810.
29. **Tanford, C.** 1961. Physical chemistry of macromolecules. John Wiley & Sons, Inc., New York.
30. **Ware, B. R., T. Raj, W. H. Flygare, J. A. Lesnaw, and M. E. Reichmann.** 1973. Molecular weights of vesicular stomatitis virus and its defective particles by laser light-scattering spectroscopy. J. Virol. 11:141–145.
31. **Wolf, K.** 1972. Diseases of fish, p. 205–221. Academic Press Inc., London.
32. **Wrigley, N. G. W.** 1968. The lattice spacing of crystalline catalse as an internal standard of length in electron microscopy. J. Ultrastruct. Res. 24:454–464.